

Electronic Supplementary Information (ESI)

Magnetic bioactive glass nano-heterostructures: a deeper insight into magnetic hyperthermia properties in the scope of bone cancer treatment

Florestan Vergnaud,^a Xavier Kesse,^a Aurélie Jacobs,^a Francis Perton,^b Sylvie Begin-Colin,^b Damien Mertz,^b Stéphane Descamps,^c Charlotte Vichery,^{*a} Jean-Marie Nedelec^a

^a Université Clermont Auvergne, Clermont Auvergne INP, CNRS, ICCF, F-63000 Clermont-Ferrand, France.

^b Institut de Physique et Chimie des Matériaux de Strasbourg (IPCMS), UMR-7504 CNRS-Université de Strasbourg, Strasbourg 67034 Cedex 2, France

^c Université Clermont Auvergne, Clermont Auvergne INP, CHU de Clermont-Ferrand, CNRS, ICCF, F-63000 Clermont-Ferrand, France.

* Corresponding author: charlotte.vichery@sigma-clermont.fr

Full-pattern matching of X-ray diffractograms

The bare magnetic NPs diffraction pattern was fitted using the Fullprof suite of programs, using a Pseudo-Voigt peak profile. The lattice parameter was determined by least-squares refinement of the corresponding d-spacings. After a correction from the instrumental line broadening (instrumental resolution function obtained from monocrystalline silicon powder), the Langford method as implemented in this Full Pattern Matching analysis allowed to discriminate between the finite size and strain effects on peaks broadening, and to obtain the average apparent crystallite size.

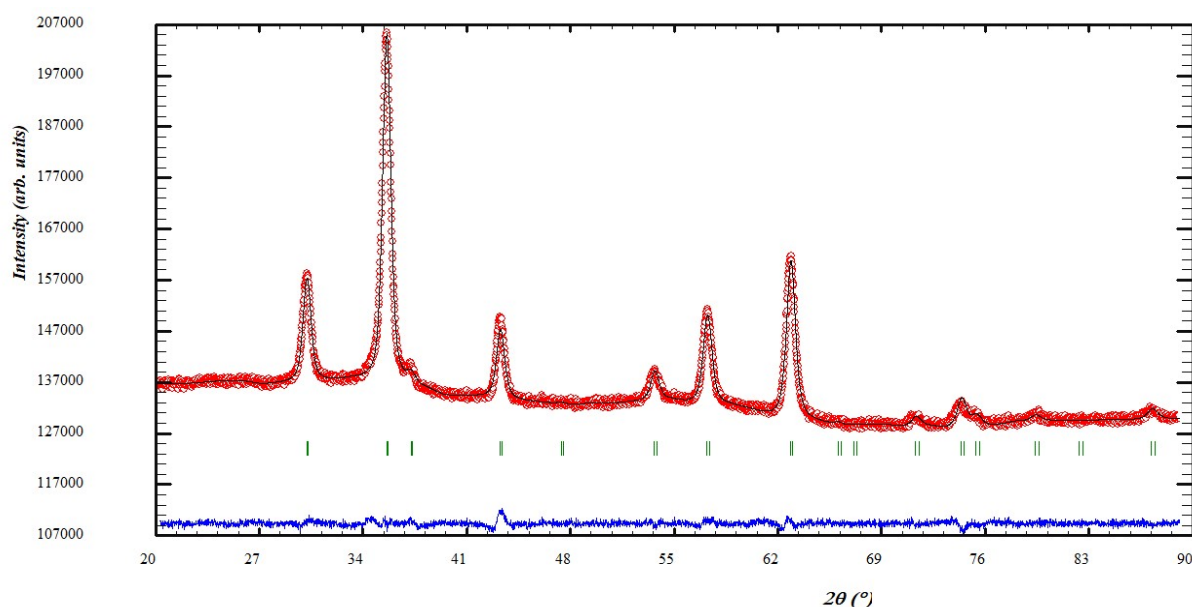


Figure S1. Experimental (red markers) and simulated (black line) diffractograms and difference between experimental and simulated values (blue line)

Morphological characterization of $\gamma\text{-Fe}_2\text{O}_3@\text{SiO}_2\text{-CaO}$ heterostructures

Representative TEM images with a significant number of particles reveal that core-shell heterostructures are rather single-core, with some NPs presenting clustered cores inside one shell. NPs agglomeration is due to the drying step and is not attributed to the synthesis.

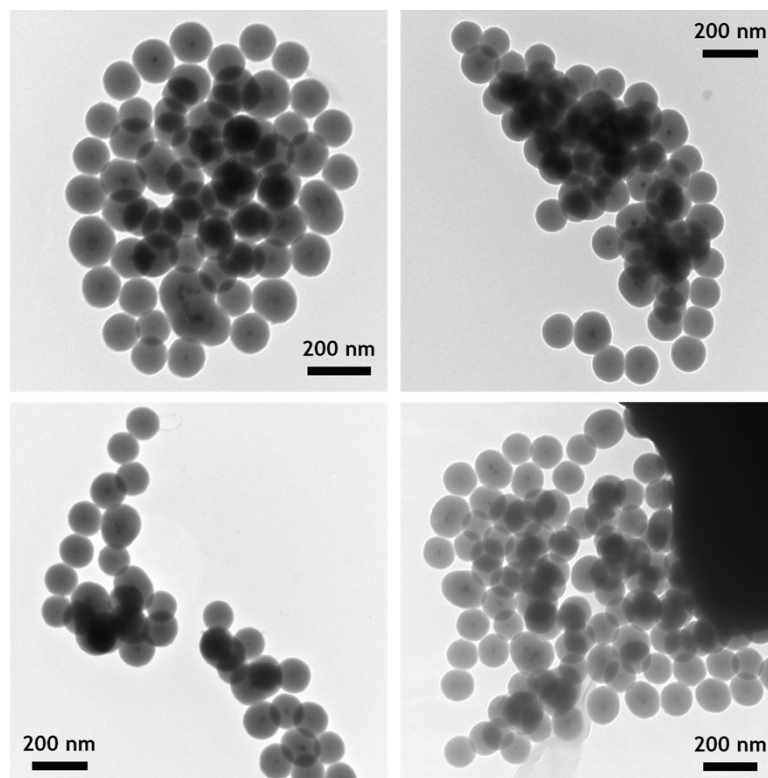


Figure S2. Representative TEM images of $\gamma\text{-Fe}_2\text{O}_3@\text{SiO}_2\text{-CaO}$ heterostructures

Nitrogen adsorption-desorption isotherm

Based on the IUPAC classification, the adsorption-desorption isotherm of the core-shell NPs (see below) is of type II, meaning that they are non-porous. The hysteresis between adsorption and desorption curves at high relative pressures can be attributed to inter-particle porosity. The average diameter d for non-porous and non-agglomerated spherical particles is related to the density ρ and the number of particles per gram N , through the formula: $(\pi/6) \cdot d^3 N \rho = 1$. Considering that the specific surface area is expressed as $S_{\text{BET}} = N\pi d^2$, the average diameter can be obtained as $d = 6000/(S_{\text{BET}} \cdot \rho)$ with d in nm, ρ in g/cm^3 and S_{BET} in m^2/g .¹ Considering a density between 1.8 and 2.2 g/cm^3 for the heterostructures (based on literature values for Stöber silica particles,² and given the low percentage of iron oxide in the sample), the theoretical mean diameter derived from S_{BET} , would range from 100 to 120 nm. This is in accordance with the size histogram (Fig. 4) and thus confirms the non-agglomerated state of the NPs.

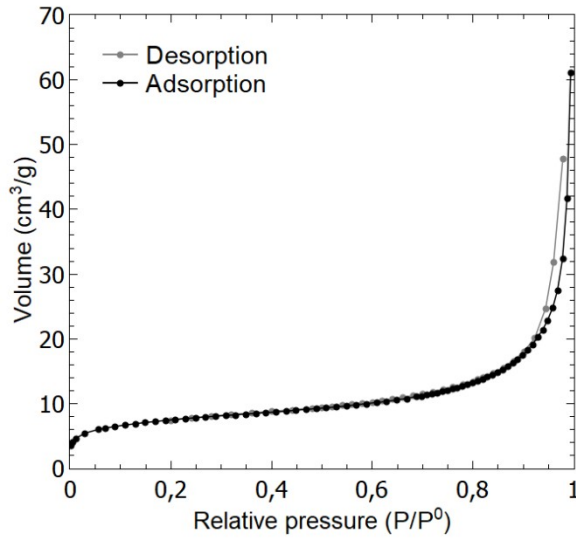


Figure S3. N₂ adsorption-desorption isotherm of heterostructured NPs

1. Dallavalle JM. Pitman Publishing Corporation; 1948.
2. Bell NC, Minelli C, Tompkins J, Stevens MM, Shard AG. *Langmuir*. 2012;28(29):10860-10872.

Hyperthermia measurements and heating power (SLP) calculation

According to the expression of SLP in the initial slope method, $\left(\frac{\Delta T}{\Delta t}\right)_{t=0}$ has to be estimated to calculate the SLP value. The temperature profiles were fitted with a second order polynomial function:

$$y = ax^2 + bx + c, \text{ where } c = 0 \text{ and } b = \left(\frac{\Delta T}{\Delta t}\right)_{t=0}$$

Table S1. Initial slope (b) and calculated SLP values of heterostructured NPs for different AMF conditions

↓ f	H ₀ →	11.9 kA/m	15.9 kA/m	23.9 kA/m
157.1 kHz		b = 0.008 ± 0.001	b = 0.015 ± 0.003	b = 0.040 ± 0.001
		SLP = 43 ± 4	SLP = 81 ± 18	SLP = 207 ± 4
303.7 kHz		b = 0.010 ± 0.001	b = 0.029 ± 0.002	b = 0.068 ± 0.004
		SLP = 54 ± 8	SLP = 153 ± 9	SLP = 354 ± 22
383.1 kHz		b = 0.019 ± 0.003	b = 0.036 ± 0.001	b = 0.078 ± 0.001
		SLP = 101 ± 13	SLP = 185 ± 6	SLP = 407 ± 6
492.9 kHz		b = 0.025 ± 0.001	b = 0.043 ± 0.001	b = 0.091 ± 0.002
		SLP = 131 ± 3	SLP = 225 ± 6	SLP = 472 ± 9
636.8 kHz		b = 0.028 ± 0.001	b = 0.051 ± 0.001	b = 0.117 ± 0.002
		SLP = 147 ± 5	SLP = 266 ± 5	SLP = 609 ± 12
768.5 kHz		b = 0.029 ± 0.005	b = 0.054 ± 0.004	b = 0.147 ± 0.015
		SLP = 152 ± 25	SLP = 282 ± 22	SLP = 767 ± 77

With $b = \Delta T/\Delta t$ ($^{\circ}\text{C}/\text{s}$) and SLP ($\text{W}/\text{g}_{\text{Fe}}$) mean values \pm standard deviation on 3 measurements

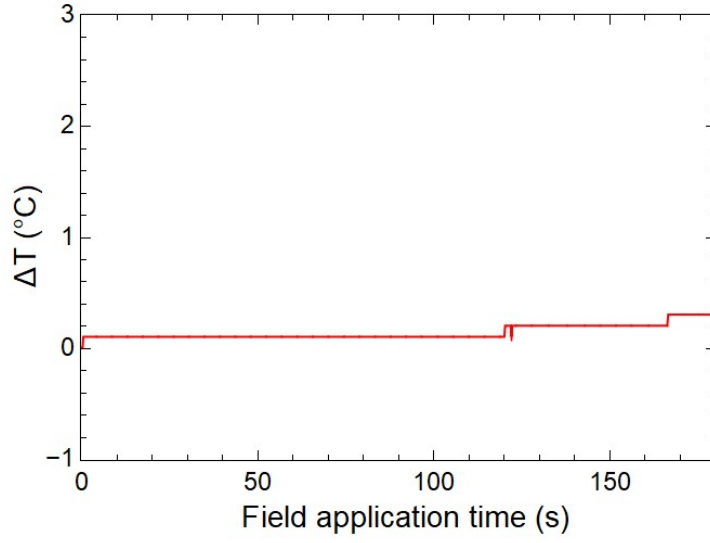


Figure S4. Temperature evolution of pure water under AMF with $H_0 = 23.9$ kA/m and $f = 768.5$ kHz

Fitting procedure to obtain the relaxation time τ_R value from experimental SLP versus AMP frequency curves

As the two parameters to be fitted (a and τ_R) are supposed to be field amplitude and frequency independent, the 3 sets of experimental SLP vs field frequency data, corresponding to the 3 different field amplitudes, were fitted with the same a and τ_R

$$SLP = aH_0^2 \cdot \frac{2\pi f^2 \tau_R}{1 + (2\pi f \tau_R)^2}$$

values using the equation

via maximization of the R^2 value :

$$R^2 = 1 - \frac{\sum_{i=1}^n (y_i - \hat{y}_i)^2}{\sum_{i=1}^n (y_i - \bar{y}_i)^2}$$

Several values of a were used to fit the experimental data with a fixed τ_R value and one R^2 was obtained for each data set ($H_0 = 11.9, 15.9$ and 23.9 kA/m) for the different a values. The value of a leading to a maximization of the product $R^2_{11.9} \times R^2_{15.9} \times R^2_{23.9}$ was selected and used to fit with the same approach the experimental data with several values of τ_R . This procedure was repeated several times until a and τ_R values converged.

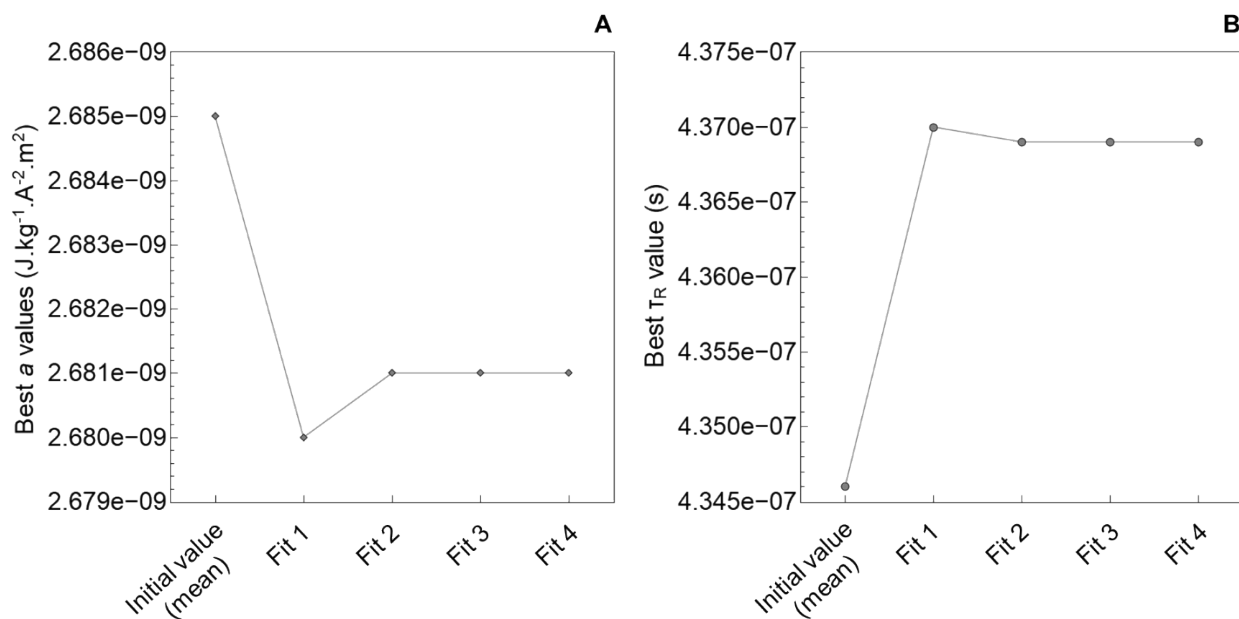


Figure S5. Best values for the constant a (A) and the relaxation time τ_R (B) after a certain number of fits using the procedure described in the main text

Hyperthermia measurements of heterostructured NPs suspended in agar gel

1 mL of $0.6 \text{ mg}_{\text{Fe}}/\text{mL}$ NPs suspended in $1 \%_{\text{wt}}$ agar showed effective heating from room temperature and did not saturate during the 15 min magnetic hyperthermia measurement.

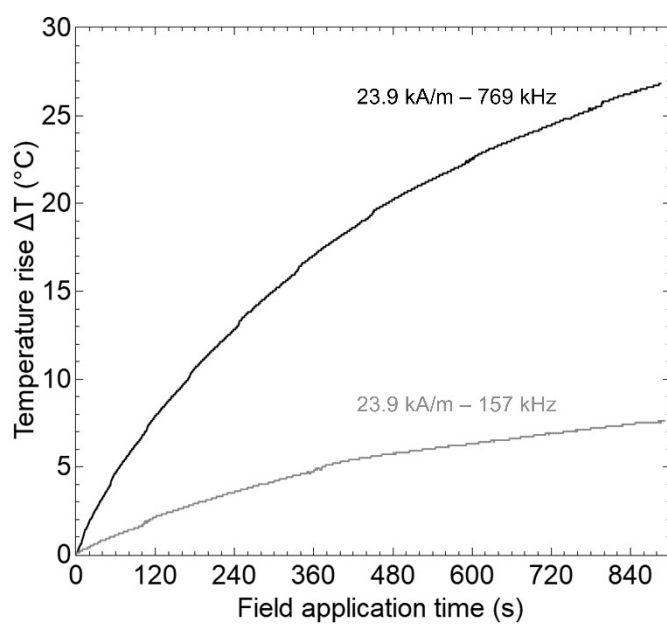


Figure S6. Temperature profiles as a function of time under different AMF parameters for heterostructured NPs dispersed in $1 \%_{\text{wt}}$ agar